

Simulation of the Indian monsoon and its variability during the last millennium

S. Polanski et al.

Simulation of the Indian monsoon and its variability during the last millennium

S. Polanski¹, B. Fallah¹, S. Prasad², and U. Cubasch¹

¹Institute of Meteorology, Freie Universität Berlin, Berlin, Germany

²German Research Center for Geosciences (GFZ), Potsdam, Germany

Received: 21 January 2013 – Accepted: 28 January 2013 – Published: 7 February 2013

Correspondence to: S. Polanski (stefan.polanski@met.fu-berlin.de)

Published by Copernicus Publications on behalf of the European Geosciences Union.

[Title Page](#)

[Abstract](#)

[Introduction](#)

[Conclusions](#)

[References](#)

[Tables](#)

[Figures](#)

[⏪](#)

[⏩](#)

[◀](#)

[▶](#)

[Back](#)

[Close](#)

[Full Screen / Esc](#)

[Printer-friendly Version](#)

[Interactive Discussion](#)

Abstract

The general circulation model ECHAM5 has been used to simulate the Indian monsoon and its variability during the Medieval Warm Period (MWP; 900–1100 AD), the Little Ice Age (LIA; 1515–1715 AD) and for recent climate (REC; 1800–2000 AD). The focus is on the analysis of external drivers and internal feedbacks leading to extreme rainfall events over India from interannual to multidecadal time scale. An evaluation of spatiotemporal monsoon patterns with present-day observation data is in agreement with other state-of-the-art monsoon modeling studies. The simulated monsoon intensity on multidecadal time scale is weakened (enhanced) in summer (winter) due to colder (warmer) SSTs in the Indian Ocean. Variations in solar insolation are the main drivers for these SST anomalies, verified by very strong temporal anticorrelations between Total Solar Irradiance and All-India-Monsoon-Rainfall in summer monsoon months. The external solar forcing is coupled and overlain by internal climate modes of the ocean (ENSO and IOD) with asynchronous intensities and lengths of periods.

In addition, the model simulations have been compared with a relative moisture index derived from paleoclimatic reconstructions based on various proxies and archives in India. In this context, the Lonar record in Central India has been highlighted and evaluated the first time. The simulated relative annual rainfall anomalies in comparison to present-day climate are in agreement (disagreement) with the reconstructed moisture index for MWP (LIA) climate.

In order to investigate the interannual monsoon variability with respect to monsoon failures, dry summer monsoon composites for 30-yr-long periods of MWP, LIA and REC have been further analysed. Within dry years of LIA, the summer rainfall over India and surrounding oceans is less than in MWP indicating stronger drying conditions due to a stronger summer solar insolation forcing coupled with variations in ENSO. To quantify the ECHAM5 simulated long-term drought conditions within Monsoon Asia, the Palmer Drought Severity Index has been additionally estimated for recent climate

CPD

9, 703–740, 2013

Simulation of the Indian monsoon and its variability during the last millennium

S. Polanski et al.

[Title Page](#)

[Abstract](#)

[Introduction](#)

[Conclusions](#)

[References](#)

[Tables](#)

[Figures](#)

[⏪](#)

[⏩](#)

[◀](#)

[▶](#)

[Back](#)

[Close](#)

[Full Screen / Esc](#)

[Printer-friendly Version](#)

[Interactive Discussion](#)



showing strong pattern correlation between global SST anomalies and EOF variability signal of the drought index, whereas the temporal relationship is weak.

1 Introduction

Based on long-term climate reconstructions derived from various well-dated proxy data (e.g. Borgaonkar et al., 2010; Fleitmann et al., 2007; Liu et al., 2009; Ponton et al., 2012; Prasad et al., 2006) the last Millennium is the best documented historical climate epoch. It can be divided into two major climate periods: the Medieval Warm Period (ca. 900–1350 AD) and the Little Ice Age (ca. 1500–1850 AD) (e.g. Graham et al., 2010; Lamb, 1965; Grove, 1988). Variations in solar insolation coupled with the remote impact of the internal dynamics of climate modes in the oceans like ENSO and Indian Ocean Dipole are some of the major drivers leading to long-term fluctuations in global temperature conditions during the last 1200 yr with the occurrence of the characteristic warm and cold periods. These thermal changes show a strong impact on global and regional climate phenomena like monsoons (Polanski et al., 2012), which are primarily formed due to seasonal and latitudinal differences in the incoming solar radiation with effects on the land-sea thermal contrast (Gadgil, 2003; Webster et al., 1998). As consequence, large-scale pressure gradients are generated including strong low-level atmospheric wind circulations (Dallmeyer et al., 2012). Monsoon systems are characterised by a strong spatiotemporal variability from multi-millennial to intraseasonal time scales (Ding, 2007; Lau et al., 2000; Wang, 2006). The Asian Monsoon System is the strongest monsoon system of the world (Clift and Plumb, 2008), which is divided into two strongly non-linear interacting subsystems: the East Asian Monsoon and the Indian Monsoon (Wang et al., 2001) affecting the livelihood of more than 2.5 billion people especially by the increased occurrence and frequency of extreme monsoon rainfall like deficient rainfall events with impacts on meteorological and agricultural drought conditions in recent times (e.g. Krishnan et al., 2009; Shaw and Nguyen, 2011; Ummenhofer et al., 2012). Therefore, the understanding of the

Simulation of the Indian monsoon and its variability during the last millennium

S. Polanski et al.

[Title Page](#)

[Abstract](#)

[Introduction](#)

[Conclusions](#)

[References](#)

[Tables](#)

[Figures](#)

[⏪](#)

[⏩](#)

[◀](#)

[▶](#)

[Back](#)

[Close](#)

[Full Screen / Esc](#)

[Printer-friendly Version](#)

[Interactive Discussion](#)



Simulation of the Indian monsoon and its variability during the last millennium

S. Polanski et al.

[Title Page](#)[Abstract](#)[Introduction](#)[Conclusions](#)[References](#)[Tables](#)[Figures](#)[⏪](#)[⏩](#)[◀](#)[▶](#)[Back](#)[Close](#)[Full Screen / Esc](#)[Printer-friendly Version](#)[Interactive Discussion](#)

large-scale mechanisms and regional spatiotemporal variations leading to extended past monsoon failures (megadroughts) is crucial for improving the Indian Monsoon forecasting and to develop proper mitigation strategies for the future. In this context a combined multi-proxy-climate model approach, as presented in HIMPAC (“Himalaya: Modern and Past Climates”; <http://www.himpac.org>) and CADY (“Central Asian Climate Dynamics”; <http://www.cady-climate.org>) projects, can be used to analyse the past monsoon climate in India within the last Millennium. Several paleoclimate studies have been already carried out to investigate drought conditions in Asia during the last Millennium as well as in present-day (e.g. Cook et al., 2010; Krishnan et al., 2009; Sinha et al., 2011b) using different multiproxy archives, observation and reanalysis data as well as climate model simulations. For instance based on new tree-ring width reconstructions, Sinha et al. (2011b) postulate episodic and widespread reoccurrences of monsoon megadroughts continued throughout the LIA, which are not clearly related to ENSO variability in the tropical Pacific Ocean as seen in present-day. Moreover, intraseasonal monsoon variability with a “break” spell dominated mode favors reduced precipitation over India along with southward retreat of ITCZ (Sinha et al., 2011b) and intensified rainfall over the Himalayan region (Gadgil, 2003). Other studies suggest that the occurrence of wet (India-Pakistan region) and dry (Bay of Bengal region) monsoon signals are in response to shifting atmospheric circulation patterns due to changes in SST and local convection (Mujumdar et al., 2012). The combination of statistical data analysis and/or climate simulations with paleoclimatic reconstruction methods has been performed in several studies (e.g. Hind et al., 2012; Jones et al., 2009; Kleinen et al., 2011; Rehfeld et al., 2012; Sundberg et al., 2012). The following study describes the monsoon variability and its large-scale physical mechanisms on different time scales with a focus on monsoon failures within the last Millennium for the Medieval Warm Period, the Little Ice Age and the recent climate respectively by an analysis of global climate model simulations with the general circulation model ECHAM5. To get a consistent view of the past climate, paleoclimatic model simulations describe the historical climate on different spatiotemporal scales by consideration

Simulation of the Indian monsoon and its variability during the last millennium

S. Polanski et al.

[Title Page](#)

[Abstract](#)

[Introduction](#)

[Conclusions](#)

[References](#)

[Tables](#)

[Figures](#)

[⏪](#)

[⏩](#)

[◀](#)

[▶](#)

[Back](#)

[Close](#)

[Full Screen / Esc](#)

[Printer-friendly Version](#)

[Interactive Discussion](#)



of external forcing parameters like solar variations, volcanoes or land cover changes derived from reconstructions. General circulation models of the atmosphere (AGCMs) are often used to simulate the large-scale atmospheric circulation (e.g. Kaspar et al., 2010) and the related monsoon circulation. Owing to the coarse horizontal resolution, global AGCMs are not able to capture regional-scale atmospheric circulation and precipitation processes, which strongly depend on the realistic simulation of the local topography (Polanski et al., 2010). Therefore, in this study a higher resolved AGCM is used to better resolve the rainfall patterns in orographically induced regions. In addition the model simulations will be compared with paleoclimatic reconstructions based on different proxies and archives in India. In this context the reconstructed climate of the well-dated Lonar record in Central India plays an important role (Anoop et al., 2012; Prasad et al., 2012). Due to its special location in the sensitive Core Monsoon Zone, the site is probably influenced by both monsoon branches: from the Arabian Sea and the Bay of Bengal. Particularly with regard to the long continuously chronology of the last 11 000 yr, the Lonar site presents a unique possibility for a comparison of long-term climate time series. Therefore, here the evaluation with climate model simulations is introduced and highlighted for the first time.

After a short introduction of the global climate model simulations, the reconstructed relative moisture index and the observation data are presented as well as different climate indices used for this study (Sect. 2). In Sect. 3 the modern spatiotemporal summer monsoon climatology is validated with observation data. Section 4 presents the simulation results for the last Millennium, in which the driving mechanisms for anomalous dry monsoon years are analysed. Further, the Palmer Drought Severity Index is calculated to quantify the monsoon failures in model data in comparison with tree-ring based drought conditions. In addition, the calculated relative annual rainfall anomalies are compared with paleoclimatic reconstructions based on the moisture index. Finally, concluding remarks summarise the main results (Sect. 5).

2 Model and data

2.1 Global climate model simulations

The general framework (Fig. 1) of the climate model simulations within the HIMPAC and CADY project for the last Millennium encompasses a three step hierarchy of model runs starting from a fully coupled atmosphere-ocean-land surface-biogeochemistry global model (Max Planck Institute for Meteorology Earth System Model (MPI-ESM)) for the entire past Millennium with 1206 model yr, a set of different ensemble members and a coarse horizontal resolution (A), an atmosphere-only general circulation model (ECHAM5) in a higher spatial resolution for three time slices with a length of 200 yr (B) and a high resolution regional climate model (COSMO-CLM) for 30 yr time slices (C). In a first step the MPI-ESM has been analysed to detect extreme wet and dry summer monsoon rainfall anomalies over India on multidecadal time scales of about 200 yr time periods to simulate them on a higher spatial resolution with ECHAM5 in a time slice mode. Later the output of the higher resolved global model will be used to identify extreme active and passive monsoon phases within the 200 yr and to drive the COSMO-CLM at its lateral and lower boundaries by dynamical downscaling over a domain covering Monsoon Asia.

2.1.1 Max Planck Institute for Meteorology Earth System Model (MPI-ESM)

All climate model simulations used in this study are based on the analysis of a set of five ensemble members of the fully coupled MPI-ESM (Jungclaus et al., 2010), which were conducted in the framework of the Integrated Project Millennium (<http://www.mad.zmaw.de/service-support/consortium-model-runs/millennium-experiments/index.html>) at the Max Planck Institute for Meteorology (MPI). The model includes different components, which are coupled with each other: ECHAM5 (European Centre, HAMBURG, version 5) (Roeckner et al., 2003): the general circulation model for the atmosphere (AGCM) and MPIOM (Max Planck Institute Ocean Model)

CPD

9, 703–740, 2013

Simulation of the Indian monsoon and its variability during the last millennium

S. Polanski et al.

Title Page

Abstract

Introduction

Conclusions

References

Tables

Figures

⏪

⏩

◀

▶

Back

Close

Full Screen / Esc

Printer-friendly Version

Interactive Discussion



Simulation of the Indian monsoon and its variability during the last millennium

S. Polanski et al.

[Title Page](#)

[Abstract](#)

[Introduction](#)

[Conclusions](#)

[References](#)

[Tables](#)

[Figures](#)

[⏪](#)

[⏩](#)

[◀](#)

[▶](#)

[Back](#)

[Close](#)

[Full Screen / Esc](#)

[Printer-friendly Version](#)

[Interactive Discussion](#)



to the highest temporal correlation of ensemble member mil0014 (0.67) for AIMR compared to the ensemble mean, three 200-yr long time slices for Medieval Warm Period (MWP; 900–1100 AD), Little Ice Age (LIA; 1515–1715 AD) and Recent Climate (REC; 1800–2000 AD) have been chosen to simulate them with the higher resolved atmosphere-only ECHAM5 model to identify the response of different horizontal resolutions of the atmospheric model component on the simulation of extreme monsoon rainfall events on multidecadal to centennial time scales and to investigate the dynamics and teleconnections leading to these events. The selection of the time slices within the prominent climatic periods for the MWP and LIA has been also done in comparison with the thermal conditions during these periods to identify the most dominant climatic signals within the last 1000 yr.

2.2 Data

2.2.1 Reconstructions

The ECHAM5 simulated rainfall changes between MWP, LIA and REC are compared with 9 reconstructed paleo-data (Bhattacharya et al., 2007; Chauhan et al., 2000; Deniston et al., 2000; Ely et al., 1999; Kar et al., 2002; Ponton et al., 2012; Prasad et al., 2012; Sinha et al., 2011a) derived from different archives like lake sediments, peat and stalagmites (see Table 1) using various proxies like pollen, isotopes, mineralogy and sedimentology. The archives are in the regions influenced by ISM and Westerlies (76° E–92° E and 16° N–32° N) encompassing also the Core Monsoon Zone in Central India as well as the northern Himalayan region (see Fig. 3). The annual relative moisture signal from the multiproxy investigations has been translated into a qualitative moisture index for a three-part scale: minus (plus) values indicate drier (wetter) conditions in each 200 yr time slice compared to the reference period. “No changes” are marked with zero values.

2.2.2 Observational and reanalysis data

The validation of modern summer monsoon rainfall patterns over land surface regions between ECHAM5 model and gridded observations has been carried out with GPCC6 reanalysis data from Global Precipitation Climatology Centre (Schneider et al., 2011) and the APHRODITE Monsoon Asia (60° E–150° E/15° S–55° N) Gridded Rainfall Data Set (Yatagai et al., 2012) for a present-day period from 1951–2000. Both observation data sets have a spatial horizontal resolution of 0.5°.

2.3 Climate indices

In order to quantify the long-term relationship between global teleconnection patterns and the AIMR in summer (JJAS) and winter (DJF) the temporal correlation between different climate indices and the AIMR has been calculated.

2.3.1 Total Solar Irradiance

The Total Solar Irradiance (TSI) is defined as the amount of the shortwave radiation emitted by the sun with a distinctive range of wavelengths (spectra) determined by the sun temperature. Total means that the solar flux has been integrated over all wavelengths (<http://www.ipcc.ch/pdf/glossary/tar-ipcc-terms-en.pdf>; <http://science.jrank.org>).

2.3.2 Oceanic Niño Index

The oceanic part of ENSO phenomenon has been analysed by calculating the Oceanic Niño Index (ONI) from NOAA/NWS/CPC (2011) based on the SST anomalies in the Niño 3.4 region (120° W–170° W and 5° S–5° N) for the pre-monsoon season from April to June (AMJ) since the highest negative correlation (–0.6) between ONI and AIMR has been identified for that season by interpretation of the MPI-ESM Millennium

CPD

9, 703–740, 2013

Simulation of the Indian monsoon and its variability during the last millennium

S. Polanski et al.

Title Page

Abstract

Introduction

Conclusions

References

Tables

Figures

⏪

⏩

◀

▶

Back

Close

Full Screen / Esc

Printer-friendly Version

Interactive Discussion



Experiment. The thresholds for El Niño and La Niña are defined by the following criteria:

El Niño: at least 5 consecutive seasons with an $ONI \geq 0.5^\circ\text{C}$.

La Niña: at least 5 consecutive seasons with an $ONI \leq 0.5^\circ\text{C}$.

5 2.3.3 Dipole Mode Index

The Dipole Mode Index (DMI) has been calculated by the difference of SST anomalies between the tropical western Indian Ocean (50°E – 70°E and 10°S – 10°N) and the tropical southeastern Indian Ocean (90°E – 110°E and 10°S – 0°S). The index oscillates between positive and negative values. A positive (negative) DMI event is characterized by warmer (cooler) than normal SSTs in the western and cooler (warmer) SSTs in the eastern basin (Clark et al., 2003).

2.3.4 North Atlantic Oscillation

The winter (DJF) station-based NAO Index (Hurrell, 1995) is estimated by the difference of normalized SLP between Lisbon, Portugal and Stykkisholmur/Reykjavik on Iceland. Positive (negative) values are associated with stronger zonal (meridional) stream in mid-latitudes, more intense (weaker) weather systems and warmer (cooler) temperatures over Western Europe.

2.3.5 Atlantic Multidecadal Oscillation

The Atlantic Multidecadal Oscillation (AMO) is generally defined as the detrended low-pass filtered annual mean SST anomalies averaged over the entire North Atlantic basin (95°W – 10°E and 0°N – 80°N) (Enfield et al., 2001).

CPD

9, 703–740, 2013

Simulation of the Indian monsoon and its variability during the last millennium

S. Polanski et al.

Title Page

Abstract

Introduction

Conclusions

References

Tables

Figures

⏪

⏩

◀

▶

Back

Close

Full Screen / Esc

Printer-friendly Version

Interactive Discussion



2.3.6 Pacific Decadal Oscillation

The Pacific Decadal Oscillation (PDO) is a SST variability mode of about 20–30 yr in the northern Pacific Ocean (120° E–240° E and 20° N–70° N). During a warm (cold) phase the Pacific becomes cool (warm) (Trenberth, 1990).

2.3.7 Palmer Drought Severity Index

The Palmer Drought Severity Index (PDSI) developed by Palmer (1965) is one of the best climatological indicators of the prolonged and abnormal periods of moisture deficiency, which can quantify the drought severity over different climates (Wells et al., 2004). Monthly PDSI has been calculated to quantify long-term drought conditions within the ECHAM5 simulations for the period from 1856 to 2000 AD overlapping with the Kaplan SST V2 data provided by the NOAA/OAR/ESRL PSD, Boulder, Colorado, USA from their web site at <http://www.esrl.noaa.gov/psd/> for further investigation of correlation between Sea Surface Temperature Anomalies (SSTA) and droughts over Monsoon Asia. The climatological dataset of available water content from global soil texture and derived water-holding capacities (Webb et al., 2000) has been used for PDSI calculations.

3 Modern summer monsoon climatology and variability

In order to evaluate the skill of the ECHAM5 simulated spatiotemporal summer monsoon patterns, in a first step the rainfall simulations have been compared with the coarse resolved MPI-ESM of Millennium Experiment (Jungclaus et al., 2010) as well as with two gridded observed rainfall data sets (Schneider et al., 2011; Yatagai et al., 2012) for a recent time period from 1951–2000. The focus is on analysing the reliability of the climate simulations with respect to different horizontal resolutions for past climate studies.

CPD

9, 703–740, 2013

Simulation of the Indian monsoon and its variability during the last millennium

S. Polanski et al.

Title Page

Abstract

Introduction

Conclusions

References

Tables

Figures

⏪

⏩

◀

▶

Back

Close

Full Screen / Esc

Printer-friendly Version

Interactive Discussion



3.1 Spatial rainfall patterns (JJAS)

Compared to GPCC6 the agreement in the climatology and interannual variability of the spatial ISM rainfall patterns over land surface regions, simulated by the higher resolved ECHAM5 model for the period from 1951–2000 (not shown), is much better than for the coarse resolved MPI-ESM, which is primary related to the more detailed representation of orographic features in the higher resolved GCM. The coarse model shows a homogeneous rainfall distribution, whereas ECHAM5 T63L31 simulates topography induced rainfall belts more realistically. Due to the characteristic modern ISM circulation with deep convection and orographic uplifting processes, intensive and long-term extended rainfall events occur especially in the windward of the Western Ghats at the Malabar Coast, at the southern slopes of the Himalayas and in the northern Bay of Bengal, which are relatively well captured by ECHAM5 even if the amount of rainfall is less than in GPCC6. Therefore, the realistic simulation of orography and small scale rainfall patterns respectively is crucial to get a better understanding of changes in rainfall distribution over short horizontal distances in a highly structured relief, which has been achieved by the higher resolved ECHAM5 model.

3.2 Temporal rainfall climatology (JJAS)

The Taylor diagram (Taylor et al., 2001) has been used to compare the simulated and observed temporal summer monsoon rainfall climatology from 1951–2000 covering a box over India (0° N– 50° N and 60° E– 12° E). First the model output and the observations have been interpolated to a coarser grid before analysing the data. Figure 4 shows a good temporal correlation and a small RMSE between the two observations as well as between the two models. The coarser resolved MPI-ESM (D) represents a slightly better agreement with GPCC6 (B) and APHRDITE (A) than ECHAM5 (C) with the increased spatial resolution. The standard deviation is also closer to GPCC6. It is believed that higher spatial resolved simulations can better capture the internal climate variations which would also limit the potential agreement between model simulations

Simulation of the Indian monsoon and its variability during the last millennium

S. Polanski et al.

Title Page

Abstract

Introduction

Conclusions

References

Tables

Figures

⏪

⏩

◀

▶

Back

Close

Full Screen / Esc

Printer-friendly Version

Interactive Discussion



due to interpolation errors, e.g. here we used the bilinear interpolation to decrease the spatial resolutions to the lowest resolved model (MPI-ESM). The temporal correlation of the two climate models and GPCC6 is about 0.6 and the centered RMSE is about 0.5 for MPI-ESM and 0.7 for ECHAM5.

In general the ECHAM5 model is able to successfully simulate the modern spatiotemporal patterns of summer monsoon rainfall climatology and variability with respect to observation data, which has been already shown in other state-of-the-art global monsoon modeling studies (e.g. Dallmeyer et al., 2010). Therefore, it can be used for further interpretation of past climate changes in the Indian Monsoon.

4 Climatic change of Indian monsoon during last millennium

4.1 Simulated rainfall changes and comparison with reconstructions

Changes in the external forcing (e.g. Total Solar Irradiance (TSI), volcanoes or orbital parameters) and in the diabatic heating source have an impact on the circulation and rainfall patterns (Dallmeyer et al., 2010). In Fig. 5 the climatological summer (JJAS; upper panel) and winter monsoon (DJF; lower panel) relative rainfall anomalies as well as differences in mean sea level pressure are illustrated for the ECHAM5 simulations during the MWP, LIA and REC time slices.

Compared to REC, for the MWP (a) summer months, ECHAM5 simulates less rainfall over most parts of western Central Asia, the northern Arabian Sea, India and the Bay of Bengal and increasing rainfall northeast of this region including the Tibetan Plateau. This dipole precipitation pattern is related to regional changes in temperature and circulation. The overall warming signal in MWP is more pronounced north of 30° N and a slight cooling is simulated in the tropics. Therefore, the intensity of temperature gradient and the position of the ITCZ are shifted to the east going along with an enhancement of EASM (not shown). Drier conditions over northern Arabian Sea and Bay of Bengal are connected to lower SSTs in the ocean basins going along with a reduction

Simulation of the Indian monsoon and its variability during the last millennium

S. Polanski et al.

Title Page

Abstract

Introduction

Conclusions

References

Tables

Figures

⏪

⏩

◀

▶

Back

Close

Full Screen / Esc

Printer-friendly Version

Interactive Discussion



Simulation of the Indian monsoon and its variability during the last millennium

S. Polanski et al.

[Title Page](#)

[Abstract](#)

[Introduction](#)

[Conclusions](#)

[References](#)

[Tables](#)

[Figures](#)

[⏪](#)

[⏩](#)

[◀](#)

[▶](#)

[Back](#)

[Close](#)

[Full Screen / Esc](#)

[Printer-friendly Version](#)

[Interactive Discussion](#)



for the three simulated time slices. Before applying the calculation for the ECHAM5 data, the different indices have been validated for present-day with observation data (not shown). The solar forcing, defined by the TSI, is the main driver for summer monsoon rainfall with a strong anticorrelation of -0.95 (-0.94 and -0.95) for MWP (LIA and REC), which is statistically significant at a 95 % confidence level. A positive (negative) solar irradiance leads to a weakening (intensification) of summer monsoon rainfall. The causal mechanisms between solar forcing and rainfall events with a focus on dry monsoon years will be described in Sect. 4.2. Especially in the summer months, the external solar forcing is coupled and overlain by internal climate modes of the ocean (ENSO and IOD) with asynchronous intensities and lengths of periods shown by anticorrelations of -0.61 (-0.57 and -0.65) for the ONI in MWP (LIA and REC) and -0.68 (-0.57 and -0.70) for the DMI in MWP (LIA and REC). Further, the correlation analysis showed, that the influence of the climate indices on the winter monsoon rainfall is much weaker, except the NAO Index has a weak positive correlation to the AIMR in winter of 0.33 (0.24 and 0.28) for MWP (LIA and REC). Whereas PDO shows a median but not significant dependency of 0.50 (0.54 and 0.54) on the AIMR in summer, the AMO mode has no correlation to the simulated AIMR.

Moisture changes during the last millennium have been described by paleoclimatic reconstructions based on a relative moisture index using different archives and proxies (Anoop et al., 2012; Bhattacharya et al., 2007; Chauhan et al., 2000; Denniston et al., 2000; Ely et al., 1999; Kar et al., 2002; Ponton et al., 2012; Prasad et al., 2012) (Fig. 6). The figure compares the ECHAM5 simulated relative annual rainfall anomalies and the reconstructed paleoclimatic moisture index between MWP, LIA and REC. Since the driving model simulations of the coarse resolved Millennium Experiment show a significant long-term increasing trend in the solar irradiance and the Meridional Overturning Circulation (MOC) in the Atlantic Basin for the last 100 yr (Zanchettin et al., 2010), the ECHAM5 simulated rainfall time series for REC had been detrended before the comparison with the rainfall anomalies of the other time slices to eliminate the long-term climate signal.

Simulation of the Indian monsoon and its variability during the last millennium

S. Polanski et al.

[Title Page](#)

[Abstract](#)

[Introduction](#)

[Conclusions](#)

[References](#)

[Tables](#)

[Figures](#)

[⏪](#)

[⏩](#)

[◀](#)

[▶](#)

[Back](#)

[Close](#)

[Full Screen / Esc](#)

[Printer-friendly Version](#)

[Interactive Discussion](#)



Especially for MWP (a) there is a good spatial agreement between the model simulation and the reconstructions. The dry (wet) rainfall signal over Central India (Himalayas) can be detected from both. However, the model and the reconstructions disagree in the LIA (b), where the model simulates relatively more rainfall over Central India and Himalayas while the reconstructions indicate a marginally drier anomaly, but the signal is not very clear and pronounced. Therefore, more sites and higher resolved climate model simulations have to be considered in the analysis to better compare the model results with respect to the inhomogeneities in the spatial rainfall distribution. The study from Dallmeyer et al. (2012) further suggests the importance of extending the analysis period of monsoon climate change to other seasons since the paleoclimate moisture reconstructions cannot simply be interpreted as indicator for summer monsoon intensity and related precipitation. It is assumed that the orbital variations lead to seasonal insolation distribution and affected the rainfall in all seasons. Therefore, the reconstructed moisture signals should not simply be correlated and explained with variations in summer insolation (Dallmeyer et al., 2012).

4.2 Dry summer monsoon composites

4.2.1 Simulated rainfall anomalies

In order to investigate the interannual summer monsoon (JJAS) variability of the last Millennium with a focus on extreme rainfall events, three 30-yr-long strong (wet) and weak (dry) monsoon composites for every 200-yr time slices of MWP, LIA and REC have been selected and compared with each other regarding their characteristic rainfall anomalies and regional and large-scale dynamical drivers. The focus of the following analysis is on dry rainfall events leading to significant monsoon failures (droughts). The selection of the anomalous dry summer monsoon years (MWP: 992–1022 AD, LIA: 1633–1663 AD and REC: 1913–1943 AD) has been done by calculation of ECHAM5 time series averaged over AIMR region (not shown). Figure 7 illustrates ECHAM5 simulated anomaly composites of summer monsoon rainfall and vertical velocity at 500 hPa

Simulation of the Indian monsoon and its variability during the last millenniumS. Polanski et al.

[Title Page](#)[Abstract](#)[Introduction](#)[Conclusions](#)[References](#)[Tables](#)[Figures](#)[⏪](#)[⏩](#)[◀](#)[▶](#)[Back](#)[Close](#)[Full Screen / Esc](#)[Printer-friendly Version](#)[Interactive Discussion](#)

in the Indian Ocean due to changes in external forcing and internal feedbacks of the surrounding oceans (see also Sect. 4.1). Figure 8 schematises the ECHAM5 estimated influence and strength of the external forcing versus internal feedbacks of the ocean on the AIMR in the summer monsoon months (JJAS) for dry (wet) monsoon years in the MWP time slice. As already discussed in Sect. 4.1, the dominant driver of summer monsoon rainfall variability are variations in the Total Solar Irradiance with even higher temporal anticorrelations of -0.98 (-0.95) for dry (wet) monsoon years on interannual than on multidecadal time scale, overlapped by nonlinear feedbacks of the oceanic internal climate modes. The ENSO phenomenon has a stronger internal feedback on the interannual rainfall anomalies than the DMI with a temporal anticorrelation of -0.70 (-0.69) in dry (wet) monsoon years, whereas the correlation between AIMR and DMI tends towards zero. Even if the same hierarchy of forcing for dry and wet monsoons is obvious, the physical mechanisms and effects leading to the formation of the characteristic interannual rainfall anomalies are reverse. These processes can be summarised as follows: positive (negative) solar irradiance leads to warming (cooling) effects of the Indian Ocean with a weakening (enhancement) of the meridional temperature gradient between the Eurasian land mass and the ocean and a weakening (intensification) of the lower-tropospheric heat low. Therefore, the moisture advection towards the continent embedded in a reduced (enhanced) southwestern low-level jet over Arabian Sea and Bay of Bengal is weaker (stronger). Finally, a weaker (stronger) convective activity going along with a lower (higher) occurrence and frequency of summer rainfall events can be simulated. Further it can be identified, that the convection is driven by large-scale moisture advection from the Indian Ocean and a strong upward motion of water vapor over land related to enhanced instability and moisture convergence, which has been already analysed in previous studies (e.g. Bhalmé et al., 1980; Krishnan et al., 2003; Polanski et al., 2010).

4.2.2 Palmer Drought Severity Index and global SST anomalies

Further the characteristic rainfall patterns in dry monsoon years have been correlated to global SST anomalies by using Empirical Orthogonal Function (EOF) Analysis to quantify the relationship between monsoon failures (droughts) on interannual time scale and global internal variability modes of the oceans. According to that, the EOF/PC1 and EOF/PC4 of the PDSI (see also Sect. 2.3.6) have been calculated within the Monsoon Asia region for the 200-yr-long ECHAM5 present-day simulation (REC) from 1800–2000 AD and later correlated with global SST anomalies from Kaplan SST V2 data for pre- and summer monsoon (MAMJJA) and winter monsoon (DJF) season between 1856 and 2000 AD. The simulation of the broad-scale monsoon failure events with robust long-term modes of spatiotemporal variability can provide deeper insights into the dynamics of Indian monsoon variability (Cook et al., 2010). Two of the EOF modes are highlighted in Fig. 9. The leading pattern accounts for 15.75% of the total field variability. Dominant same-sign loadings are detected over India, South and Southeast Asia with opposite sign loadings over Tibetan Plateau, northern Pakistan, Pamir and Tien-Shan Mountains, which are in well agreement with the DEOF1 of the reconstructed PDSI from Cook et al. (2010). It indicates the simulated dipole rainfall patterns in dry monsoon years between India and Tibetan Plateau seen especially in LIA. Moreover the temporal expansion of this mode (PC1) correlated well with the hemispherically SST anomalies of interdecadal variability in the Pacific Ocean, seen also in Cook et al. (2010). The late-20th century trend toward drier conditions and weaker monsoons over India and Southeast Asia (see Fig. 9) can be explained by similar mechanisms leading to droughts in MWP and LIA. The EOF4 pattern accounts for 4.5% of the total field variance with strong positive loadings over China and northeastern Asia and negative loadings over India. The PC4 of this mode is positively correlated with Indian Ocean SST anomalies, which are related to the DMI and tends to more positive PDSI values during the last 200 yr. The ENSO–PDSI relationship in

the ECHAM5 simulation is relatively weak (not shown), whereas the internal dynamics of IOD is more pronounced.

5 Conclusions

The general circulation model ECHAM5 has been used to simulate the Indian Monsoon Variability within the last Millennium. The focus has been on 200-yr-long time slices of the Medieval Warm Period (900–1100 AD), the Little Ice Age (1515–1715 AD) and the recent climate (1800–2000 AD). The evaluation of spatiotemporal monsoon patterns with present-day observation data is in agreement with other state-of-the-art monsoon modeling studies. Due to the better horizontal resolution of the ECHAM5 model, the rainfall patterns especially in the orographic regions can be captured more realistically. However, high resolution regional climate models are necessary as an additional tool to improve the skill for the simulation of small scale processes in comparison with observed data.

The multidecadal rainfall changes have been simulated and compared for MWP and LIA according to the recent climate. ECHAM5 calculated a weakening (enhancement) in summer (winter) monsoon rainfall due to colder (warmer) SSTs in the Indian Ocean. Variations in the external solar insolation are the main drivers for these SST anomalies, shown by very strong temporal anticorrelations of -0.95 (-0.94 and -0.95) for MWP (LIA and REC) between the Total Solar Irradiance and the All-India-Monsoon-Rainfall in the summer monsoon months. A positive (negative) solar irradiance leads to a weakening (intensification) of summer monsoon rainfall. The external solar forcing is further coupled and overlain by internal climate modes of the ocean shown by anticorrelations of -0.61 (-0.57 and -0.65) for the ONI in MWP (LIA and REC) and -0.68 (-0.57 and -0.70) for the DMI in MWP (LIA and REC) with asynchronous intensities and lengths of periods. Moreover, the correlation analysis depicted a weaker influence of the climate indices on the winter monsoon rainfall.

Simulation of the Indian monsoon and its variability during the last millennium

S. Polanski et al.

[Title Page](#)

[Abstract](#)

[Introduction](#)

[Conclusions](#)

[References](#)

[Tables](#)

[Figures](#)

[⏪](#)

[⏩](#)

[◀](#)

[▶](#)

[Back](#)

[Close](#)

[Full Screen / Esc](#)

[Printer-friendly Version](#)

[Interactive Discussion](#)



Simulation of the Indian monsoon and its variability during the last millennium

S. Polanski et al.

[Title Page](#)

[Abstract](#)

[Introduction](#)

[Conclusions](#)

[References](#)

[Tables](#)

[Figures](#)

[⏪](#)

[⏩](#)

[◀](#)

[▶](#)

[Back](#)

[Close](#)

[Full Screen / Esc](#)

[Printer-friendly Version](#)

[Interactive Discussion](#)



India and the continental regions north of Arabian Sea (+0.5 K) compared to LIA. The positive anomalies in vertical velocity at 500 hPa represent the regions with strongest convective activity, which are associated with a strong moisture convergence as well as a strong upward motion in the middle troposphere. In MWP the strongest convective activity occurs over India and Arabian Sea, whereas the convection is reduced over these parts in LIA as a result of shifted atmospheric circulation patterns. Changes in the distribution of rainfall anomalies can be attributed to shifting regional atmospheric circulation patterns driven by modified regional SST anomalies in the Indian Ocean due to changes in external forcing and internal feedbacks of the surrounding oceans. The dominant drivers of summer monsoon rainfall variability are variations in the Total Solar Irradiance with high temporal anticorrelations of -0.98 (-0.95) for dry (wet) monsoon years, overlapped by nonlinear feedbacks of the oceanic internal climate modes. The ENSO phenomenon has a stronger internal feedback on the interannual rainfall anomalies than the DMI with a temporal anticorrelation of -0.70 (-0.69) in dry (wet) monsoon years. Even if the same hierarchy of forcing for dry and wet monsoons is obvious, the physical mechanisms and effects leading to the formation of the characteristic interannual rainfall anomalies are reverse. These processes can be summarised as follows: positive (negative) solar irradiance leads to warming (cooling) effects of the Indian Ocean with a weakening (enhancement) of the meridional temperature gradient between the Eurasian land mass and the ocean and a weakening (intensification) of the lower-tropospheric heat low. Therefore, the moisture advection towards the continent embedded in a reduced (enhanced) southwestern low-level jet over Arabian Sea and Bay of Bengal is weaker (stronger). Finally, a weaker (stronger) convective activity going along with a lower (higher) occurrence and frequency of summer rainfall events can be simulated.

Furthermore the characteristic rainfall patterns during years of weak monsoon activity have been correlated to global SST anomalies by using EOF Analysis to quantify the relationship between droughts on interannual time scale and global internal variability modes of the oceans for the present-day simulation from 1800–2000 AD. Dominant

Simulation of the Indian monsoon and its variability during the last millennium

S. Polanski et al.

[Title Page](#)

[Abstract](#)

[Introduction](#)

[Conclusions](#)

[References](#)

[Tables](#)

[Figures](#)

[⏪](#)

[⏩](#)

[◀](#)

[▶](#)

[Back](#)

[Close](#)

[Full Screen / Esc](#)

[Printer-friendly Version](#)

[Interactive Discussion](#)



same-sign loadings are detected over India, South and Southeast Asia with opposite sign loadings over Tibetan Plateau, northern Pakistan, Pamir and Tien-Shan Mountains, which are in well agreement with the DEOF1 of the reconstructed PDSI from Cook et al. (2010). Moreover the temporal expansion of this mode (PC1) correlated well with the hemispherically SST anomalies of interdecadal variability in the Pacific Ocean, seen also in Cook et al. (2010).

Acknowledgements. This research was supported and funded by the DFG research group FOR 1380 “HIMPAC – Himalaya Modern and Past Climates” and the BMBF joint research project “CADY – Central Asian Climate Dynamics”. The authors thank the individual HIMPAC and CADY teams for permanent support and fruitful discussions, especially Daniel J. Befort for providing a figure. Further we thank Raghavan Krishnan and Milind Mujumdar from Indian Institute of Tropical Meteorology (IITM), Pune for enhanced collaboration and interesting discussions within HIMPAC and for their hospitality during a research stay at IITM. The MPI-ESM data from Millennium Experiment had been supplied by the Max Planck Institute for Meteorology (MPI-M) Hamburg. The authors thank Johann H. Jungclaus, MPI-M Hamburg for MPI-ESM data from Millennium-Experiment and Stephan J. Lorenz, MPI-M Hamburg for many helpful advices in SST interpolation and running ECHAM5 model.

References

- Anoop, A., Prasad, S., Plessen, B., Basavaiah, N., Gaye, B., Naumann, R., Menzel, P., Weise, S., and Brauer, A.: Palaeoenvironmental implications of evaporative Gaylussite crystals from Lonar Lake, Central India, *J. Quaternary Sci.*, under review, 2012.
- Bhalme, H. N. and Mooley, D. A.: Large-scale droughts/floods and monsoon circulation, *Mon. Weather Rev.*, 108, 1197–1211, 1980.
- Bhattacharya, A, Sharma, J., Shah, S. K., and Chaudhary, V.: Climatic changes during the last 1800 yrs BP from Paradise Lake, Sela Pass, Arunachal Pradesh, Northeast Himalaya, *Curr. Sci. India*, 93, 983–987, 2007.
- Borgaonkar, H. P., Sikdera, A. B., Rama, S., and Panta, G. B.: El Niño and related monsoon drought signals in 523-year-long ring width records of teak (*Tectona grandis* L.F.) trees from south India, *Paleogeogr. Paleoclimatol.*, 285, 74–84, 2010.

Simulation of the Indian monsoon and its variability during the last millennium

S. Polanski et al.

[Title Page](#)

[Abstract](#)

[Introduction](#)

[Conclusions](#)

[References](#)

[Tables](#)

[Figures](#)

[⏪](#)

[⏩](#)

[◀](#)

[▶](#)

[Back](#)

[Close](#)

[Full Screen / Esc](#)

[Printer-friendly Version](#)

[Interactive Discussion](#)



- Chauhan, M.S, Mazari, R. K., and Rajagopalan, G.: Vegetation and climate in upper Spiti region, Himachal Pradesh during late Holocene, *Curr. Sci. India*, 79, 373–377, 2000.
- Clark, C. O., Webster, P. J., and Cole, J.: Interdecadal variability of the relationship between the Indian Ocean zonal mode and East African coastal rainfall anomalies, *J. Climate*, 16, 548–554, 2003.
- 5 Clift, P. D. and Plumb, R. A.: *The Asian Monsoon: Causes, History and Effects*, Cambridge University Press, Cambridge, 2008.
- Cook, E. R., Anchukaitis, K. J., Buckley, B. M., D'Arrigo R. D., Jacoby, G. C., and Wright, W. E.: Asian monsoon failure and megadrought during the last millennium, *Science*, 328, 486–489, 2010.
- 10 Dallmeyer, A., Claussen, M., and Otto, J.: Contribution of oceanic and vegetation feedbacks to Holocene climate change in monsoonal Asia, *Clim. Past*, 6, 195–218, doi:10.5194/cp-6-195-2010, 2010.
- Dallmeyer, A., Claussen, M., Wang, Y., and Herzschuh, U.: Spatial variability of Holocene changes in the annual precipitation pattern: a model-data synthesis for the Asian monsoon region, *Clim. Dynam.*, 39, 18 pp., doi:10.1007/s00382-012-1550-6, 2012.
- 15 Denniston, R. F. and Gonzalez, L. A.: Speleothem evidence for changes in Indian summer monsoon precipitation over the last ~2300 years, *Quaternary Res.*, 53, 196–202, 2000.
- Ding, Y. H.: The variability of the Asian summer monsoon, *J. Meteorol. Soc. Jpn.*, 85, 21–54, 2007.
- 20 Ely, L. L., Enzel, Y., Baker, V. R., Kale, V. S., and Mishra, S.: Changes in the magnitude and frequency of late Holocene monsoon floods on the Narmada River, central India, *Geol. Soc. Am. Bull.*, 108, 1134–1148, 1996.
- Enfield, D. B., Mestas-Nuñez, A. M., and Trimble, P. J.: The Atlantic multidecadal oscillation and its relation to rainfall and river flows in the continental US, *Geophys. Res. Lett.*, 28, 2077–2080, 2001.
- 25 Fleitmann, D., Burns, S. J., Mangini, A., Mudelsee, M., Kramers, J., Villa, I., Neff, U., Subbary, A.-A., Buettner, A., Hippler, D., and Matter, A.: Holocene ITCZ and Indian monsoon dynamics recorded in stalagmites from Oman and Yemen (Socotra), *Quaternary Sci. Rev.*, 26, 170–188, 2007.
- 30 Gadgil, S.: The Indian monsoon and its variability, *Annu. Rev. Earth Pl. Sc.*, 31, 429–467, 2003.

Simulation of the Indian monsoon and its variability during the last millennium

S. Polanski et al.

[Title Page](#)

[Abstract](#)

[Introduction](#)

[Conclusions](#)

[References](#)

[Tables](#)

[Figures](#)

[⏪](#)

[⏩](#)

[◀](#)

[▶](#)

[Back](#)

[Close](#)

[Full Screen / Esc](#)

[Printer-friendly Version](#)

[Interactive Discussion](#)



Graham, N. E., Ammann, C. M., Fleitmann, D., Cobb, K. M., and Luterbacher, J.: Support for global climate reorganization during the “Medieval Climate Anomaly”, *Clim. Dynam.*, 37, 1217–1245, doi:10.1007/s00382-010-0914-z, 2010.

Grove, J. M.: *The Little Ice Age*, Menthuen, London, 1988.

Hind, A., Moberg, A., and Sundberg, R.: Statistical framework for evaluation of climate model simulations by use of climate proxy data from the last millennium – Part 2: A pseudo-proxy study addressing the amplitude of solar forcing, *Clim. Past*, 8, 1355–1365, doi:10.5194/cp-8-1355-2012, 2012.

Hurrell, J. W.: Decadal trends in the North Atlantic oscillation: regional temperatures and precipitation, *Science*, 269, 676–679, doi:10.1126/science.269.5224.676, 1995.

Jones, P. D., Briffa, K. R., Osborn, T. J., Lough, J. M., van Ommen, T. D., Vinther, B. M., Luterbacher, J., Wahl, E. R., Zwiers, F. W., Mann, M. E., Schmidt, G. A., Ammann, C. M., Buckley, B. M., Cobb, K. M., Esper, J., Goosse, H., Graham, N., Jansen, E., Kiefer, T., Kull, C., Küttel, M., Mosley-Thompson, E., Overpeck, J. T., Riedwyl, N., Schulz, M., Tudhope, A. W., Villalba, R., Wanner, H., Wolff, E., and Xoplaki, E.: High-resolution paleoclimatology of the last millennium: a review of current status and future prospects, *Holocene*, 19, 3–49, 2009.

Jungclauss, J. H., Lorenz, S. J., Timmreck, C., Reick, C. H., Brovkin, V., Six, K., Segsneider, J., Giorgetta, M. A., Crowley, T. J., Pongratz, J., Krivova, N. A., Vieira, L. E., Solanki, S. K., Klocke, D., Botzet, M., Esch, M., Gayler, V., Haak, H., Raddatz, T. J., Roeckner, E., Schnur, R., Widmann, H., Claussen, M., Stevens, B., and Marotzke, J.: Climate and carbon-cycle variability over the last millennium, *Clim. Past*, 6, 723–737, doi:10.5194/cp-6-723-2010, 2010.

Kar, R., Ranhotra, P. S., Bhattacharyya, A., and Sekar, B.: Vegetation vis-a-vis climate and glacial fluctuations of the Gangotri glacier since the last 2000 years, *Curr. Sci. India*, 82, 347–351, 2002.

Kaspar, F., Prömmel, K., and Cubasch, U.: Impacts of tectonic and orbital forcing on East African climate: a comparison based on global climate model simulations, *Int. J. Earth Sci.*, 99, 1677–1686, 2010.

Kleinen, T., Tarasov, P., Brovkin, V., Andreev, A., and Stebich, M.: Comparison of modeled and reconstructed changes in forest cover through the past 8000 years: Eurasian perspective, *Holocene*, 21, 723–734, 2011.

Krishnan, R., Mujumdar, M., Vaidya, V., Ramesh, K. V., and Satyan, V.: The abnormal Indian summer monsoon of 2000, *J. Climate*, 16, 1177–1194, 2003.

Simulation of the Indian monsoon and its variability during the last millennium

S. Polanski et al.

[Title Page](#)

[Abstract](#)

[Introduction](#)

[Conclusions](#)

[References](#)

[Tables](#)

[Figures](#)

[⏪](#)

[⏩](#)

[◀](#)

[▶](#)

[Back](#)

[Close](#)

[Full Screen / Esc](#)

[Printer-friendly Version](#)

[Interactive Discussion](#)



- Krishnan, R., Kumar, V., Sugi, M., and Yoshimura, J.: Internal feedbacks from monsoon-midlatitude interactions during droughts in the Indian summer monsoon, *J. Atmos. Sci.*, 66, 553–578, 2009.
- Lamb, H. H.: The early medieval warm epoch and its sequel, *Paleogeogr. Paleoclimatol.*, 1, 13–37, 1965.
- Lau, K. M., Kim, K. M., and Yang, S.: Dynamical and boundary forcing characteristics of regional components of the Asian summer monsoon, *J. Climate*, 13, 2461–2482, 2000.
- Liu, X., Dong, H., Yang, X., Herzschuh, U., Zhang, E., Stuetz, J.-B. W., and Wang, Y.: Late Holocene forcing of the Asian winter and summer monsoon as evidenced by proxy records from the northern Qinghai-Tibetan Plateau, *Earth Planet. Sci. Lett.*, 280, 276–284, 2009.
- Marsland, S. J., Haak, H., JungCLAUS, J. H., Latif, M., and Röske, F.: The Max-Planck-Institute global ocean/sea ice model with orthogonal curvilinear coordinates, *Ocean Model.*, 5, 91–127, 2003.
- Mujumdar, M., Preethi, B., Sabin, T. B., Karumuri, A., Saeed, S., Pai, D. S., and Krishnan, R.: The Asian summer monsoon response to the La Niña event of 2010, *Meteorol. Appl.*, 19, 216–225, doi:10.1002/met.1301, 2012.
- NOAA/NWS/CPC: Oceanic Nino Index. NOAA National Weather Service, Center for Climate Prediction, 5200 Auth Road, Camp Springs, Maryland 20746, USA, http://www.cpc.ncep.noaa.gov/products/analysis_monitoring/ensostuff/ensoyears.shtml, 2011.
- NOAA/OAR/ESRL PSD: Kaplan SST V2 data, Boulder, Colorado, USA, <http://www.esrl.noaa.gov/psd/> (last access: 5 February 2013), 1998.
- Palmer, W. C.: *Meteorological Drought*, Res. Pap., No. 45, US Weather Bureau, Washington D.C., USA, 58 pp., 1965.
- Polanski, S., Rinke, A., and Dethloff, K.: Validation of the HIRHAM-Simulated Indian Summer Monsoon Circulation, *Adv. Meteorol.*, 2010, 14 pp., doi:10.1155/2010/415632, 2010.
- Polanski, S., Rinke, A., Dethloff, K., Lorenz, S. J., Wang, Y., and Herzschuh, U.: Simulation of the mid-Holocene Indian summer monsoon circulation with a regional climate model, *Open Atmos. Sci. J.*, 6, 42–48, doi:10.2174/1874282301206010042, 2012.
- Ponton, C., Giosan, L., Eglinton, T. I., Fuller, D. Q., Johnson, J. E., Kumar, P., and Collett, T. S.: Holocene aridification of India, *Geophys. Res. Lett.*, 39, L03704, doi:10.1029/2011GL050722, 2012.
- Prasad, S. and Enzel, Y.: Holocene paleoclimates of India, *Quaternary Res.*, 66, 442–453, 2006.

Simulation of the Indian monsoon and its variability during the last millennium

S. Polanski et al.

[Title Page](#)

[Abstract](#)

[Introduction](#)

[Conclusions](#)

[References](#)

[Tables](#)

[Figures](#)

[⏪](#)

[⏩](#)

[◀](#)

[▶](#)

[Back](#)

[Close](#)

[Full Screen / Esc](#)

[Printer-friendly Version](#)

[Interactive Discussion](#)



- Prasad, S., Basavaiah, N., Anoop, A., Strecker, M. R., Krishnan, R., Priya, P., Leckebusch, G. C., Riedel, N., Menzel, P., Deendayalan, K., Mishra, P. K., Sarkar, S., Bookhagen, B., Brauer, A., Cubasch, U., Gaye, B., Goswami, B. N., Haug, G. H., Helle, G., Kurths, J., Lücke, A., Marwan, N., Nowaczyk, N., Plessen, B., Riedel, F., Sachse, D., Schleser, G. H., Stebich, M., Tarasov, P., Weise, S., Wiesner, M., Wilkes, H., Yousuf, A. R., Befort, D. J., Borgaonker, H., Breitenbach, S., Demske, D., Goswami, B., Hanf, F., Jehangir, A., Leipe, C., Polanski, S., and Wild, S. B.: Regional variability in the Indian summer monsoon realm: a modern overview and Holocene reconstruction from the Lonar Lake, Central India, *Quaternary Res.*, under revision, 2012.
- Raddatz, T. J., Reick, C. H., Knorr, W., Kattge, J., Roeckner, E., Schnur, R., Schnitzler, K.-G., Wetzol, P., and Jungclaus, J. H.: Will the tropical land biosphere dominate the climate-carbon cycle feedback during the twenty-first century?, *Clim. Dynam.*, 29, 565–574, 2007.
- Rehfeld, K., Breitenbach, S. F. M., Marwan, N., and Kurths, J.: Late Holocene Asian Summer Monsoon dynamics from small but complex networks of paleoclimate data, *Clim. Dynam.*, 39, 17 pp., doi:10.1007/s00382-012-1448-3, 2012.
- Roeckner, E., Bäuml, G., Bonaventura, L., Brokopf, R., Esch, M., Giorgetta, M., Hagemann, S., Kirchner, I., Kornbluh, L., Manzini, E., Rhodin, A., Schlese, U., Schulzweida, U., and Tompkins, A.: The atmospheric general circulation model ECHAM 5 PART 1: Model description, Tech. rep., Max-Planck-Institute for Meteorology, Bundesstr. 53, 20146 Hamburg, Germany, 2003.
- Schneider, U., Becker, A., Finger, P., Meyer-Christoffer, A., Rudolf, B., and Ziese, M.: GPCP Full Data Reanalysis Version 6 at 0.5°: Monthly Land-Surface Precipitation from Rain-Gauges built on GTS-based and Historic Data, Global Precipitation Climatology Centre, Deutscher Wetterdienst, Offenbach (Main), doi:10.5676/DWD_GPCP/FD_M_V6_050, 2011.
- Shaw, R. and Nguyen, H.: Droughts in Asian Monsoon Region, *Community, Environment and Disaster Risk Management*, Vol. 8, Emerald Books, Kyoto University, Kyoto, Japan, UK, 2011.
- Sinha, A., Berkelhammer, M., Stott, L., Mudelsee, M., Cheng, H., and Biswas, J.: The leading mode of Indian summer monsoon precipitation variability during the last millennium, *Geophys. Res. Lett.*, 38, L15703, doi:10.1029/2011GL047713, 2011a.
- Sinha, A., Stott, L., Berkelhammer, M., Cheng, H., Lawrence Edwards, R., Buckley, B., Aldenderfer, M., and Mudelsee, M.: A global context for megadroughts in monsoon Asia during the past millennium, *Quaternary Sci. Rev.*, 30, 47–62, 2011b.

Simulation of the Indian monsoon and its variability during the last millennium

S. Polanski et al.

[Title Page](#)

[Abstract](#)

[Introduction](#)

[Conclusions](#)

[References](#)

[Tables](#)

[Figures](#)

[⏪](#)

[⏩](#)

[◀](#)

[▶](#)

[Back](#)

[Close](#)

[Full Screen / Esc](#)

[Printer-friendly Version](#)

[Interactive Discussion](#)



Sundberg, R., Moberg, A., and Hind, A.: Statistical framework for evaluation of climate model simulations by use of climate proxy data from the last millennium – Part 1: Theory, *Clim. Past*, 8, 1339–1353, doi:10.5194/cp-8-1339-2012, 2012.

Taylor, K. E.: Summarizing multiple aspects of model performance in a single diagram, *J. Geophys. Res.*, 106, 7183–7192, doi:10.1029/2000JD900719, 2001.

Trenberth, K. E.: Recent observed interdecadal climate changes in the northern hemisphere, *B. Am. Meteorol. Soc.*, 71, 988–993, 1990.

Ummenhofer, C. C., D'Arrigo, R. D., Anchukaitis, K. J., Buckley, B. M., and Cook, E. R.: Links between Indo-Pacific climate variability and drought in the Monsoon Asia Drought Atlas, *Clim. Dynam.*, 39, 16 pp., doi:10.1007/s00382-012-1458-1, 2012.

Wang, B.: *The Asian Monsoon*, Springer/Praxis Publishing Co, Berlin, 2006.

Wang, B., Wu, R., and Lau, K. M.: Interannual variability of the Asian summer monsoon: contrasts between the Indian and the Western North Pacific-East Asian Monsoon, *J. Climate*, 14, 4073–4090, 2001.

Webb, R. W., Rosenzweig, C. E., and Levine, E. R.: Global Soil Texture and Derived Water-Holding Capacities, data set, available online under <http://www.daac.ornl.gov> (last access: 5 February 2013), Oak Ridge National Laboratory Distributed Active Archive Center, Oak Ridge, Tennessee, USA, 2000.

Webster, P. J., Magana, V. O., Palmer, T. N., Shukla, J., Tomas, R. T., Yanai, M., and Yasunari, T.: Monsoons: processes, predictability and the prospects of prediction, *J. Geophys. Res.*, 103, 14451–14510, 1998.

Wells, N., Goddard, S., and Hayes, M. J.: A Self-Calibrating Palmer Drought Severity Index, *J. Climate*, 17, 2335–2351, 2004.

Wetzel, P., Maier-Reimer, E., Botzet, M., Jungclaus, J. H., Keenlyside, N., and Latif, M.: Effects of ocean biology on the penetrative radiation in a coupled climate model, *J. Climate*, 19, 3973–3987, 2006.

Yatagai, A., Kamiguchi, O., Arakawa, A., Hamada, N., Yasutomi, N., and Kitoh, A.: APHRODITE: constructing a long-term daily gridded precipitation dataset for Asia based on a dense network of rain gauges, *B. Am. Meteorol. Soc.*, 93, 1401–1415, doi:10.1175/BAMS-D-11-00122.1, 2012.

Zanchettin, D., Rubino, A., and Jungclaus, J. H.: Intermittent multidecadal-to-centennial fluctuations dominate global temperature evolution over the last millennium, *Geophys. Res. Lett.*, 37, L14702, doi:10.1029/2010GL043717, 2010.

Simulation of the Indian monsoon and its variability during the last millennium

S. Polanski et al.

Table 1. Paleoclimatic records from India used in this study. Records are listed from north to south.

No	Name	ϕ ($^{\circ}$ N)	λ ($^{\circ}$ E)	Archive	Proxy	Reference
1	Sitikher bog, Spiti	32.30	77.43	Peat Bog	Pollen	Chauhan et al. (2000)
2	Gangotri	31.00	79.00	Sediment	Pollen	Kar et al. (2002)
3	Nepal	28.00	84.00	Stalagmite	Laminae thickness	Denniston et al. (2000)
4	Paradise Lake	27.30	92.06	Lake core	Pollen	Bhattacharya et al. (2007)
5	Narmada basin	23.00	77.43	Sediment	Flood deposit	Ely et al. (1999)
6	Lonar	19.51	76.00	Lake sediment	Geochemistry	Prasad et al. (2012)
7	Dandak	19.00	82.00	Stalagmite	$\delta^{18}\text{O}$ Isotope	Sinha et al. (2011a)
8	Jhumar	18.52	81.52	Stalagmite	$\delta^{18}\text{O}$ Isotope	Sinha et al. (2011a)
9	Godavari	16.00	83.00	Marine Core	Bioisotopes	Ponton et al. (2012)

Title Page

Abstract

Introduction

Conclusions

References

Tables

Figures

⏪

⏩

◀

▶

Back

Close

Full Screen / Esc

Printer-friendly Version

Interactive Discussion

Simulation of the Indian monsoon and its variability during the last millennium

S. Polanski et al.

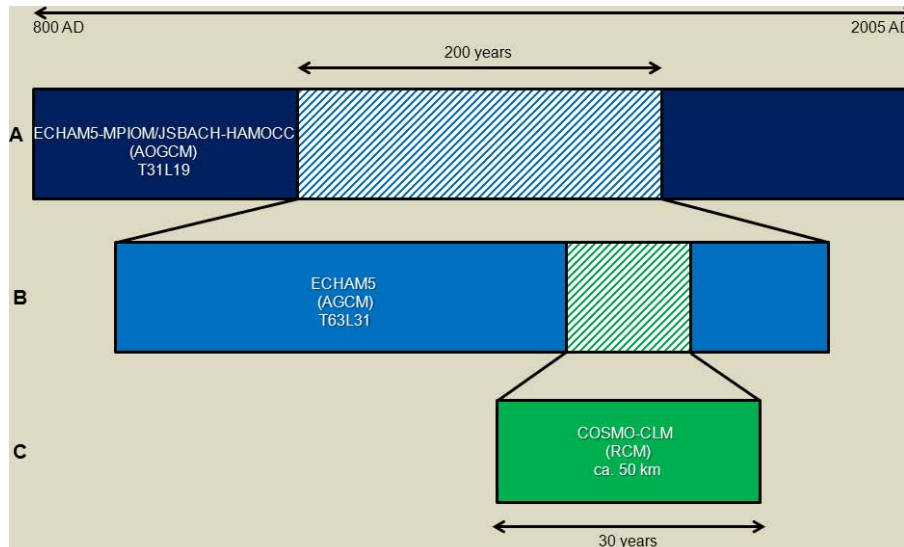


Fig. 1. Conceptual simplified framework of global (dark and light blue) and regional (green) climate simulations in HIMPAC and CADY project for the last Millennium 800–2005 AD. A – Millennium Experiment using fully coupled AOGCM in T31L19 spatial resolution (ECHAM5). B – Atmosphere-only 200 yr – time slices experiments using ECHAM5 Model in T63L31 horizontal resolution. C – High resolution regional climate model simulations with COSMO-CLM in a 50 km spatial resolution for 30-yr-time slices.

Title Page

Abstract

Introduction

Conclusions

References

Tables

Figures

⏪

⏩

◀

▶

Back

Close

Full Screen / Esc

Printer-friendly Version

Interactive Discussion

Simulation of the Indian monsoon and its variability during the last millennium

S. Polanski et al.

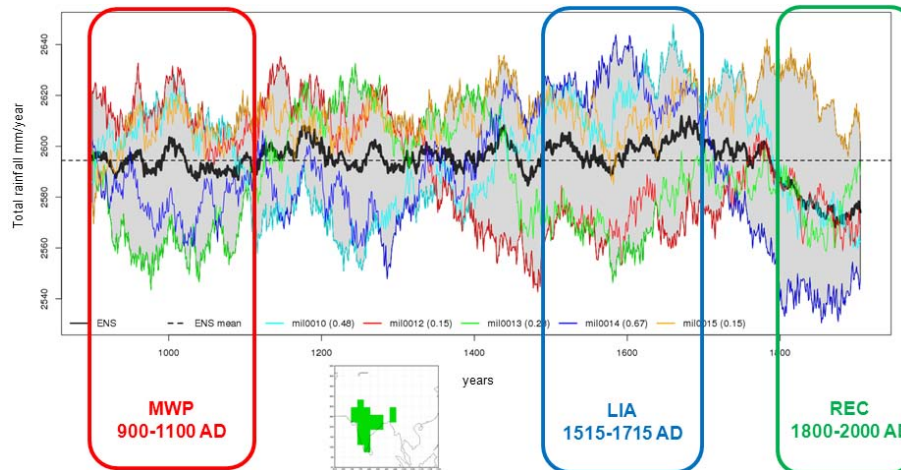


Fig. 2. Annual total rainfall in mm yr^{-1} as 200 yr running mean for five ensemble members mil0010 – mil0015 of Millennium Experiment using ECHAM5/MPIOM-JSBACH/HAMOC in T31L19 horizontal resolution (ECHAM5); 800–2005 AD averaged over AIMR (All India Monsoon Rainfall) grid boxes (small figure). The ensemble mean is shown as black solid line. The climatological mean of all ensemble members is represented by the dashed black line. The selection of time slices for the ECHAM5 simulations in T63L31 are shown by the boxes for the Medieval Warm Period (MWP; 900–1100 AD) in red, the Little Ice Age (LIA; 1515–1715 AD) in blue and the Recent Climate Period (REC; 1800–2000 AD) in green. The selection has been done according to the highest temporal correlation of ensemble member mil0014 (temporal correlation = 0.67; dark blue solid line) to the ensemble mean and the characteristic warm and cold temperature signals during MWP and LIA.

[Title Page](#)
[Abstract](#)
[Introduction](#)
[Conclusions](#)
[References](#)
[Tables](#)
[Figures](#)
[⏪](#)
[⏩](#)
[◀](#)
[▶](#)
[Back](#)
[Close](#)
[Full Screen / Esc](#)
[Printer-friendly Version](#)
[Interactive Discussion](#)

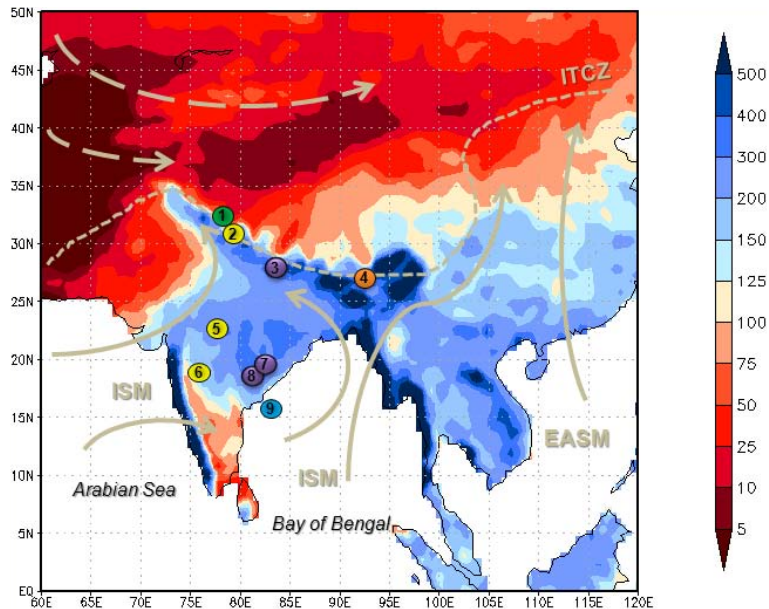


Fig. 3. Study area with climatological land surface summer monsoon rainfall (JJAS) for GPCC5 data set from 1901–2009 (mm; shaded colours), generalized summer wind directions of the Indian Summer Monsoon (ISM) and East Asian Summer Monsoon (EASM; light grey solid arrows), the Westerlies and the position of the ITCZ are shown in light grey dashed arrows and the spatial coverage of the Indian paleoclimatic records considered in this study as numbered dots. Numbers of the nodes were assigned according to the geographical coordinates of the respective study site and furthermore refer to the entries in Table 1. Sites that are at close proximity might show displaced to prevent overlap of the dots and labels. Colours of the dots indicate the type of archive: green – peat bog, yellow – sediment sites, orange – lake core, purple – stalagmites and blue – marine core.

Simulation of the Indian monsoon and its variability during the last millennium

S. Polanski et al.

Title Page

Abstract Introduction

Conclusions References

Tables Figures

⏪ ⏩

◀ ▶

Back Close

Full Screen / Esc

Printer-friendly Version

Interactive Discussion



Simulation of the Indian monsoon and its variability during the last millennium

S. Polanski et al.

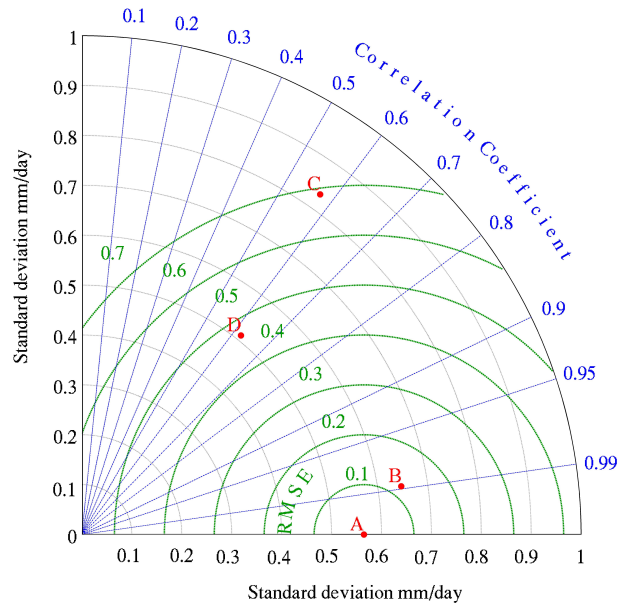


Fig. 4. Taylor diagram for rainfall time series analysis between observation data: APHRODITE (A) and GPCC6 (B) and climate model simulations: ECHAM5 Model in T63L31 spatial resolution (C) and MPI-ESM realization mil0014 with ECHAM5 Model in T31L19 spatial resolution (D) for summer monsoon (JJAS) 1951–2000.

Title Page

Abstract

Introduction

Conclusions

References

Tables

Figures

⏪

⏩

◀

▶

Back

Close

Full Screen / Esc

Printer-friendly Version

Interactive Discussion

Simulation of the Indian monsoon and its variability during the last millennium

S. Polanski et al.

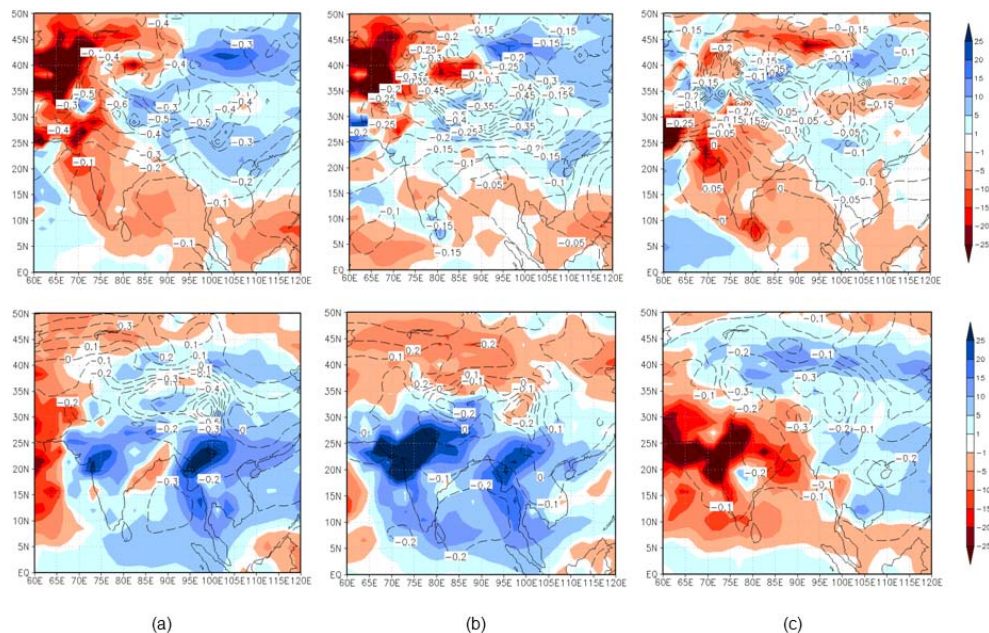


Fig. 5. Anomalies of precipitation (%; colours) and mean sea level pressure (hPa; black contour lines) for ECHAM5 in summer monsoon (JJAS; upper panel) and winter monsoon (DJF; lower panel) “MWP minus REC” (a), “LIA minus REC” (b) and “MWP minus LIA” (c).

Title Page

Abstract

Introduction

Conclusions

References

Tables

Figures

⏪

⏩

◀

▶

Back

Close

Full Screen / Esc

Printer-friendly Version

Interactive Discussion

Simulation of the Indian monsoon and its variability during the last millennium

S. Polanski et al.

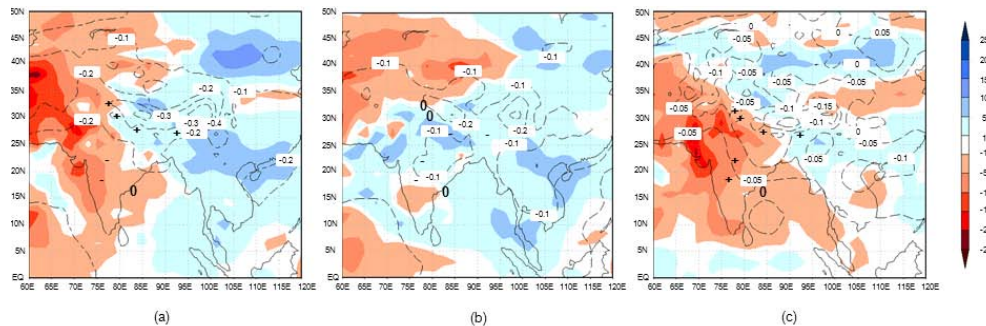


Fig. 6. Annual precipitation anomaly (%; colours) and mean sea level pressure anomalies (hPa; black contour lines) for ECHAM5 Model and reconstructed moisture index (symbols: “+” wetter, “-” drier and “0” no changes; dimensionless;) for “MWP minus REC” (a), “LIA minus REC” (b) and “MWP minus LIA” (c).

Title Page

Abstract

Introduction

Conclusions

References

Tables

Figures

⏪

⏩

◀

▶

Back

Close

Full Screen / Esc

Printer-friendly Version

Interactive Discussion

Simulation of the Indian monsoon and its variability during the last millennium

S. Polanski et al.

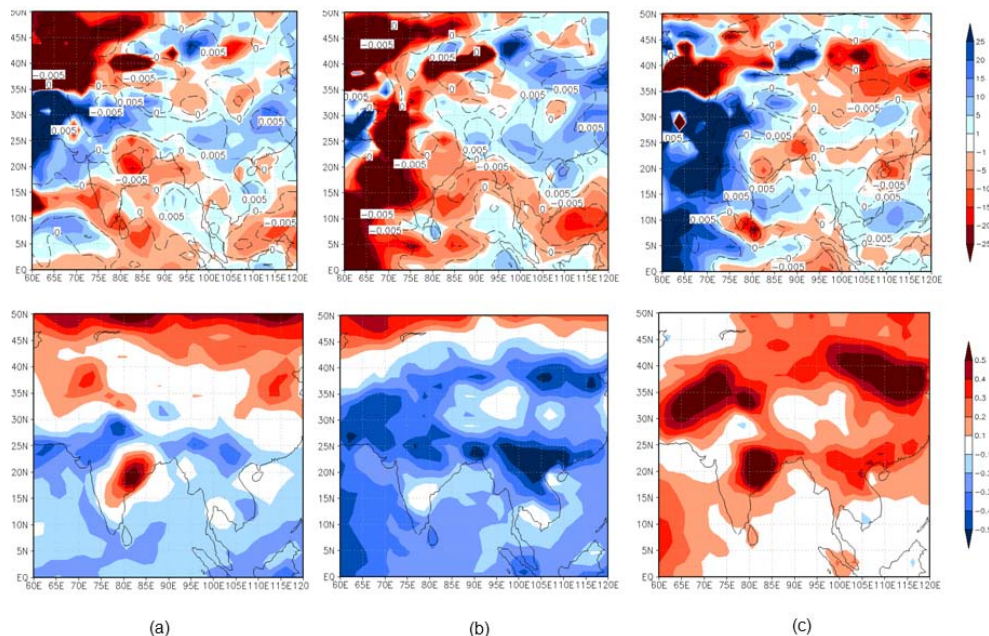


Fig. 7. Anomalies of precipitation “dry monsoons” (%; colours) and vertical velocity (ω) at 500 hPa “dry monsoons” (Pa/s; green contour lines) for ECHAM5 T63L31 shown in upper panel. Differences in 2 m-air-temperature “dry monsoons” (K; colours) for ECHAM5 shown in lower panel for “MWP minus REC” (a), “LIA minus REC” (b) and “MWP minus LIA” (c); summer monsoon (JJAS).

Title Page

Abstract

Introduction

Conclusions

References

Tables

Figures

⏪

⏩

◀

▶

Back

Close

Full Screen / Esc

Printer-friendly Version

Interactive Discussion

Simulation of the Indian monsoon and its variability during the last millennium

S. Polanski et al.

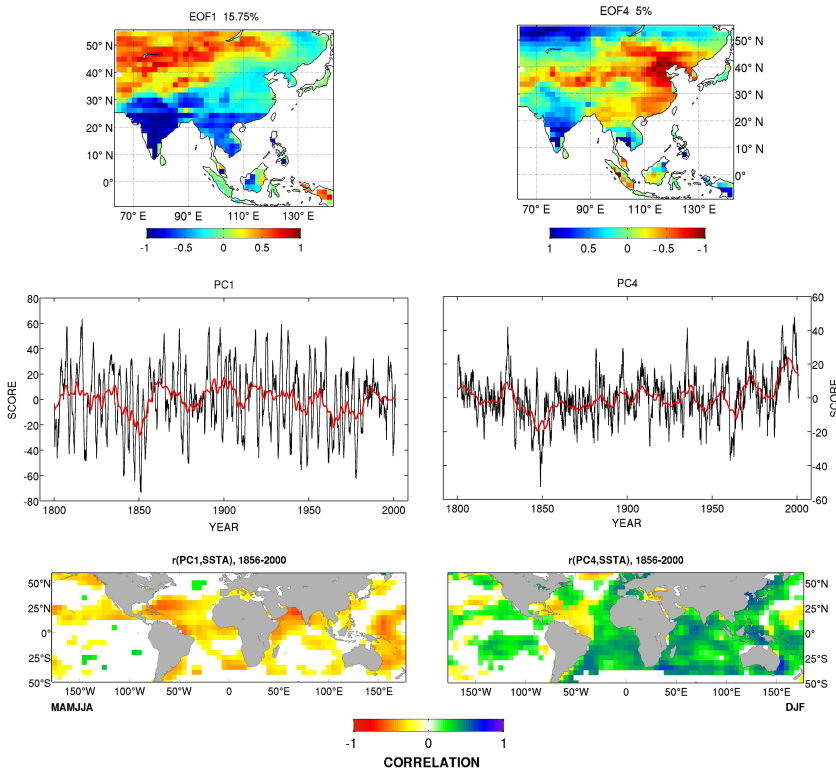


Fig. 9. Spatiotemporal patterns of the PDSI from 1800–2000 AD. Empirical orthogonal function (EOF) analysis of the PDSI with two distinct modes (EOF1 and EOF4) is shown here. Middle panels show the time series expansion (PCs, principal components) of the corresponding spatial modes in the top row. In the lower row, Pearson correlations with Sea Surface Temperature Anomalies (SSTA) and EOF/PC1 are simultaneous with the monsoon and pre-monsoon season (MAMJJA), whereas the SSTA patterns for EOF/PC4 are for the previous winter (DJF) season. Only correlation values significant at 95% confidence level are shown.